Geophysical Research Letters

Supporting Information for

Historical and Projected changes in the Southern Hemisphere surface westerlies

Rishav Goyal[1,2,*], Alex Sen Gupta[1,2], Martin Jucker[1,2], Matthew H. England[1,2]

1. Climate Change Research Centre, University of New South Wales, NSW, 2052 Australia

2. ARC Centre of Excellence for Climate Extremes, University of New South Wales, NSW, Australia

Contents of this file

[*]*Corresponding author: rishav.goyal@unsw.edu.au*

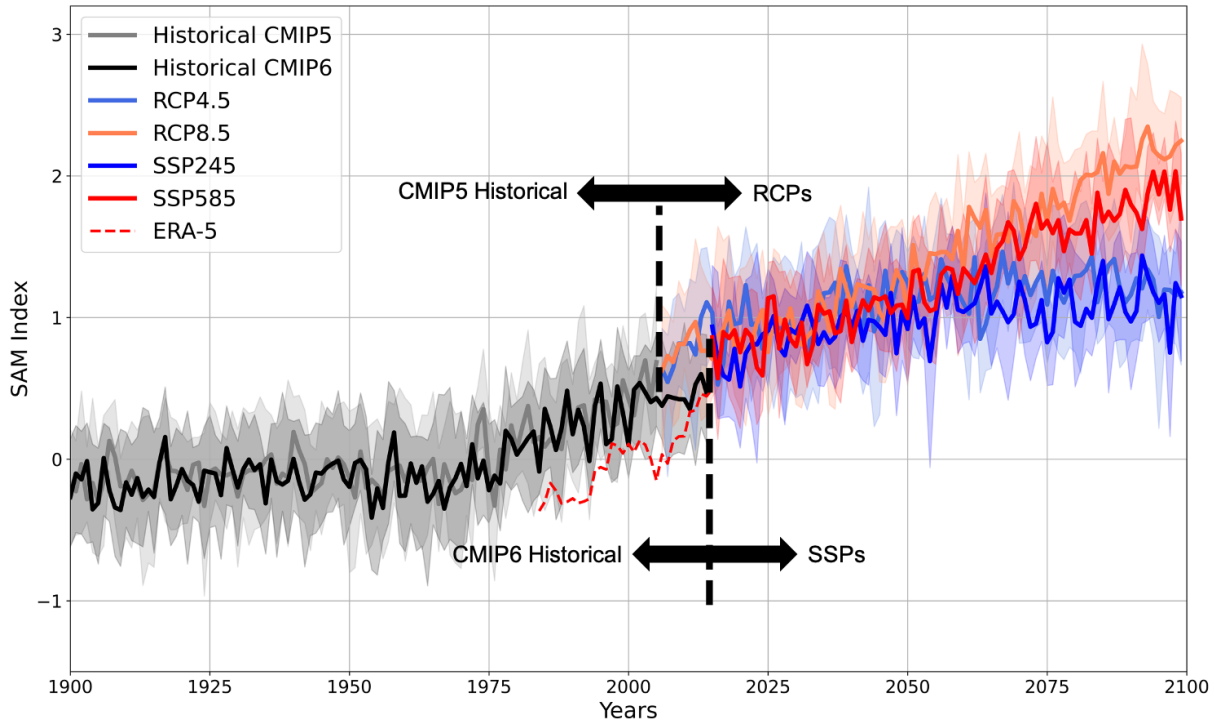

Figure S1 | Southern Annular Mode (SAM) index in CMIP5, CMIP6 models and reanalysis. SAM index is defined as the difference in the normalized zonal mean sea level pressure between 40°S and 65°S. Thick grey and black lines respectively represent the SAM index for CMIP5 and CMIP6 multi-model mean for historical period (1900-2005 for CMIP5 and 1900-2014 for CMIP6). Thick light blue and orange lines represent the multi-model mean for RCP4.5 and RCP8.5 scenarios of CMIP5 respectively. Thick blue and red lines respectively represent the multi-model mean for SSP245 and SSP585 scenario of CMIP6. Shading around the multi-model mean shows the inter-quartile range from multiple CMIP5 and CMIP6 models. Thin orange line represents 5-year running mean SAM index calculated from ERA-5 reanalysis.

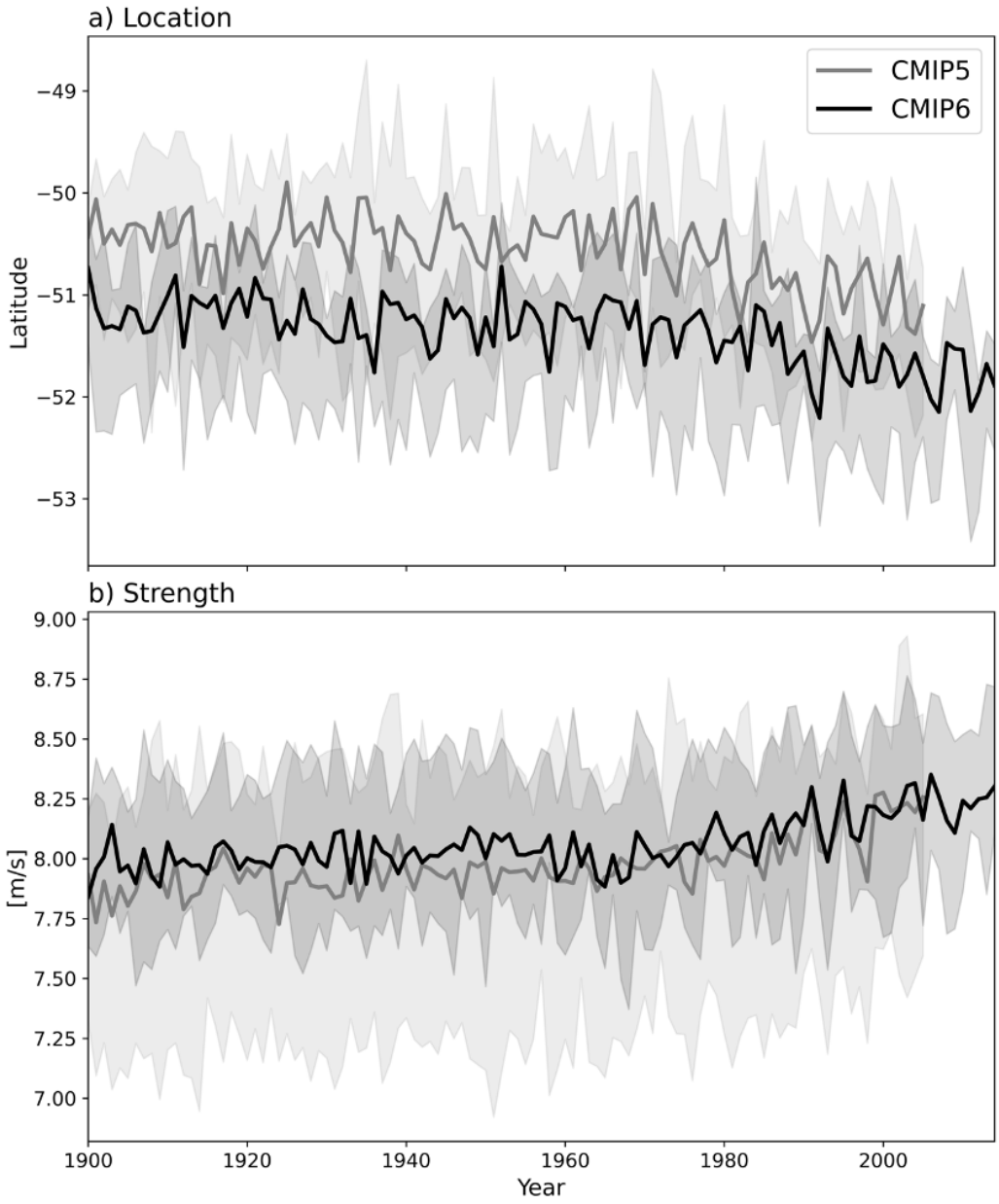

Figure S2 | Zonal mean westerly jet location (panel a) and strength (panel b) in models from common modelling groups from CMIP5 and CMIP6. Details about the models used is given in table S1 and S2.

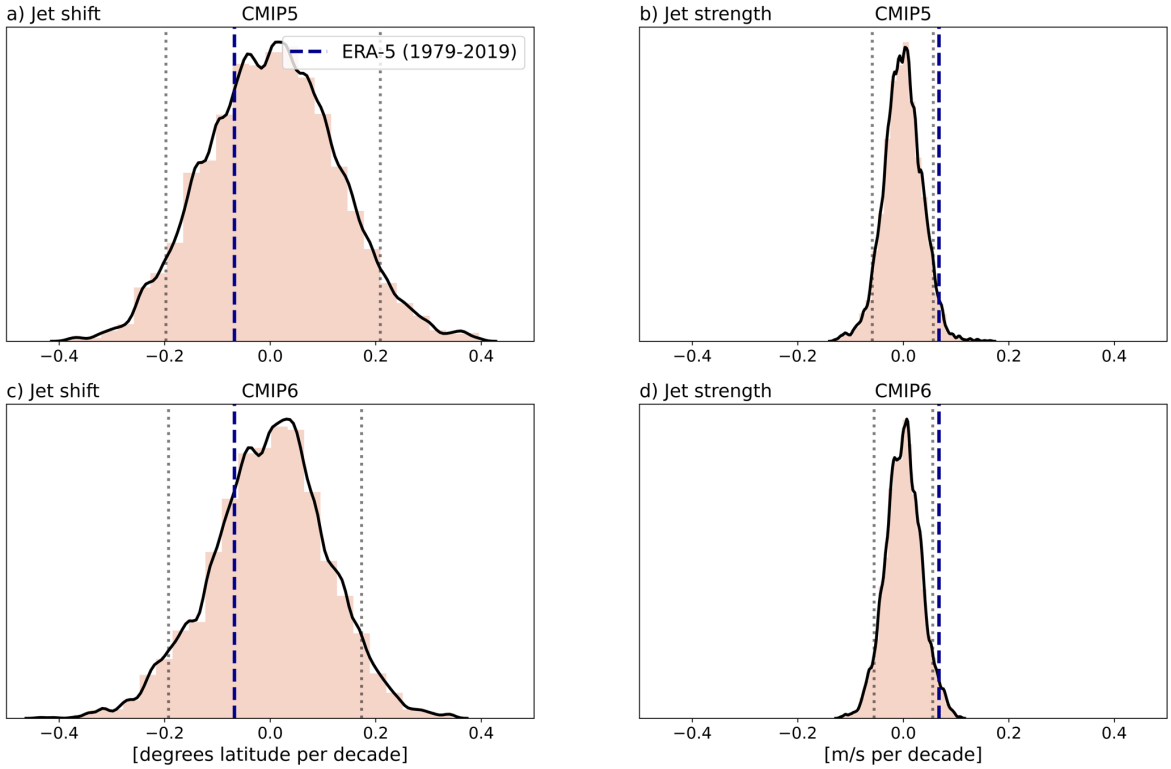

Figure S3 | Histogram represents the probability density function of 41-year annual mean trends calculated from pre-industrial control simulations from 28 CMIP5 and 23 CMIP6 models (200 years for each model). Monte Carlo method is used to calculate the trend over a random chunk of 41 years of data from 200-year simulation of each model and the process is repeated 10,000 times for each model. All the 41-year trends from each model (10,000 for each model) are then concatenated and probability density function is plotted. Dashed blue line represents the trend calculated from ERA5 reanalysis over the current observational time period (1979-2019). Dotted black lines represent 5^{th} and 95^{th} percentile (i.e. bounds for 90% confidence) of the density function. The trends calculated from the reanalysis are significant at 90% confidence if the blue dashed line does not fall between the two dotted black lines.

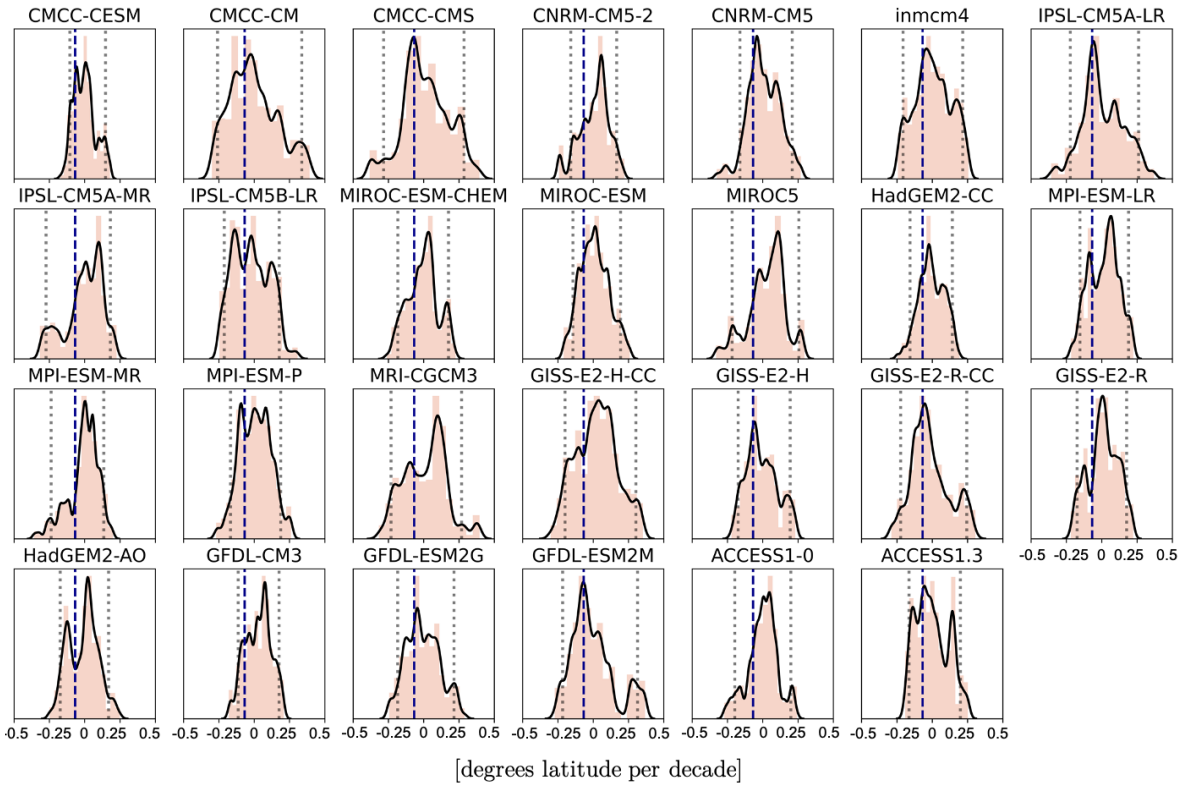

Figure S4 | Histogram represents the probability density function of 41-year annual mean trends in the zonal mean location of SH westerlies calculated from the pre-industrial control simulations from 27 CMIP5 models (200 years for each model). Monte Carlo method is used to calculate the trend over a random chunk of 41 years of data from 200-year simulation of each model and the process is repeated 10,000 times for each model. Dashed blue line represents the trend calculated from ERA5 reanalysis over the current observational time period (1979-2019). Dotted black lines represent 5th and 95th percentile (i.e. bounds for 90% confidence) of the density function. The trends calculated from the reanalysis are significant at 90% confidence if the blue dashed line does not fall between the two dotted black lines.

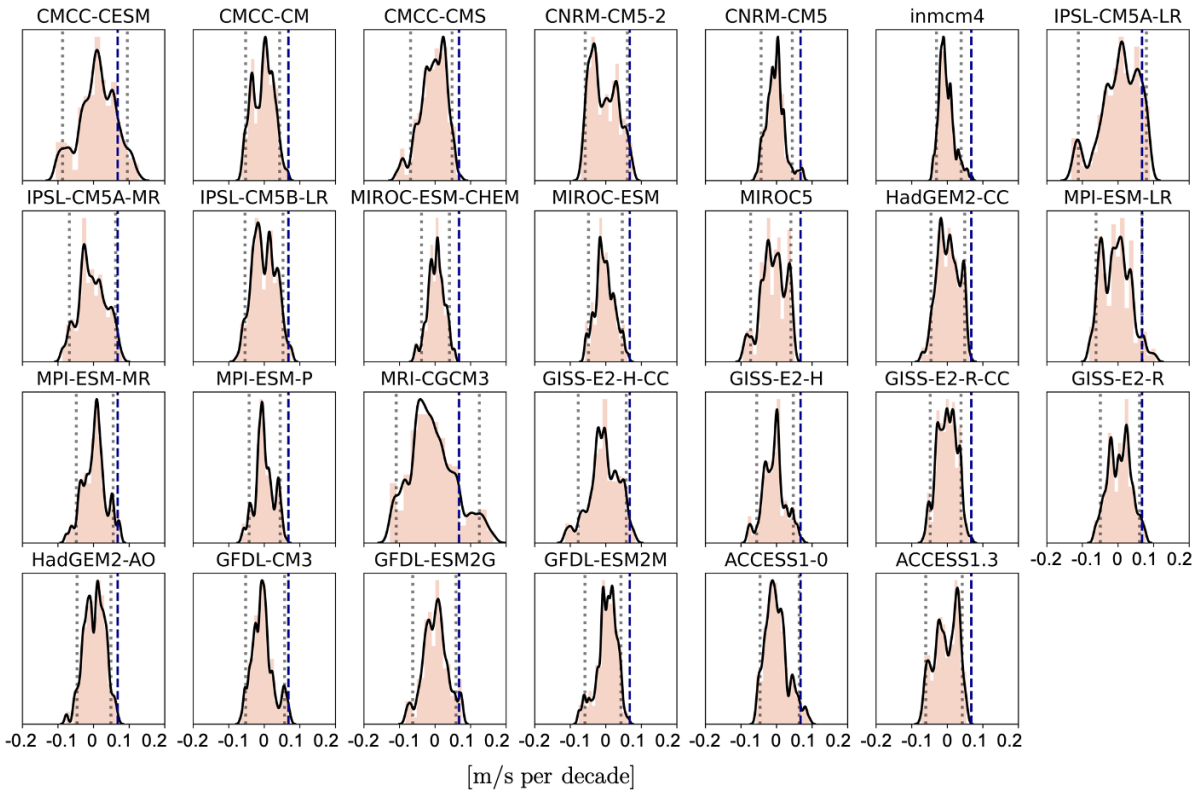

Figure S5 | Histogram represents the probability density function of 41-year annual mean trends in the zonal mean strength of SH westerlies calculated from the pre-industrial control simulations from 27 CMIP5 (200 years for each model). Monte Carlo method is used to calculate the trend over a random chunk of 41 years of data from 200-year simulation of each model and the process is repeated 10,000 times for each model. Dashed blue line represents the trend calculated from ERA5 reanalysis over the current observational time period (1979-2019). Dotted black lines represent 5th and 95th percentile (i.e. bounds for 90% confidence) of the density function. The trends calculated from the reanalysis are significant at 90% confidence if the blue dashed line does not fall between the two dotted black lines.

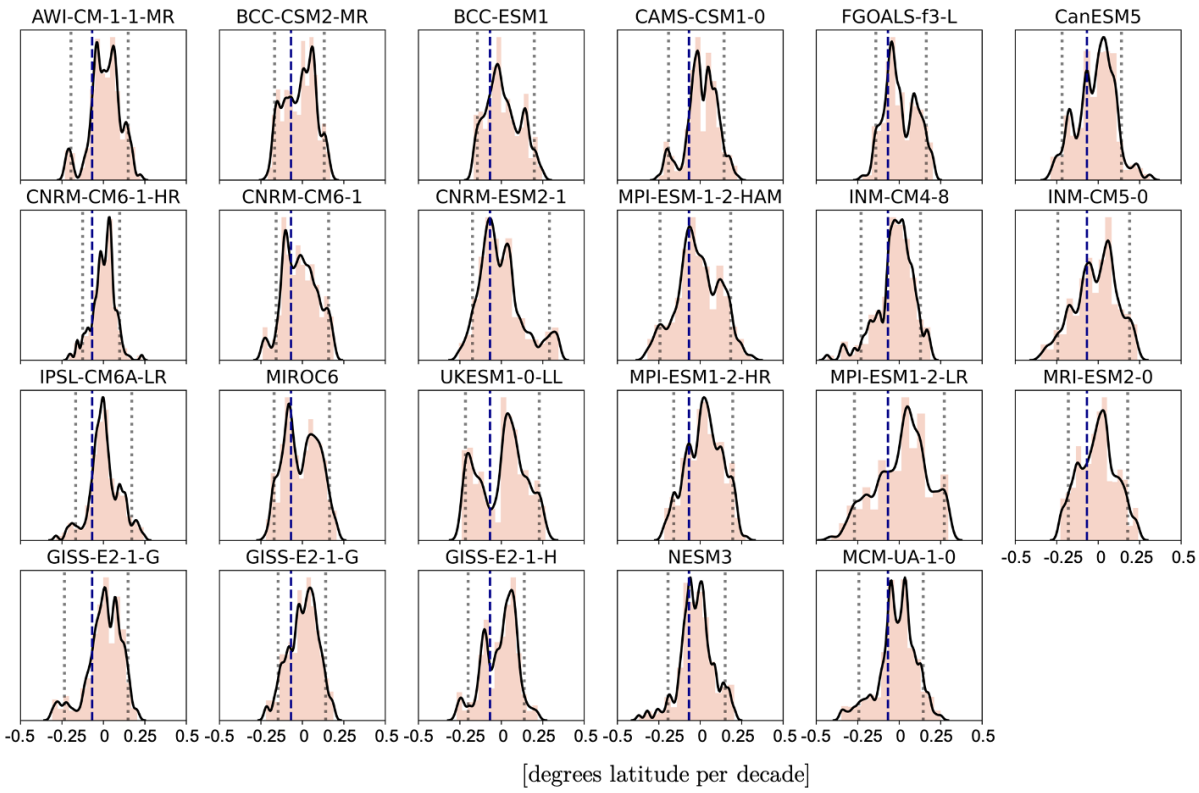

Figure S6 | Histogram represents the probability density function of 41-year annual mean trends in the zonal mean location of SH westerlies calculated from the pre-industrial control simulations from 23 CMIP6 models (200 years for each model). Monte Carlo method is used to calculate the trend over a random chunk of 41 years of data from 200-year simulation of each model and the process is repeated 10,000 times for each model. Dashed blue line represents the trend calculated from ERA5 reanalysis over the current observational time period (1979-2019). Dotted black lines represent 5th and 95th percentile (i.e. bounds for 90% confidence) of the density function. The trends calculated from the reanalysis are significant at 90% confidence if the blue dashed line does not fall between the two dotted black lines.

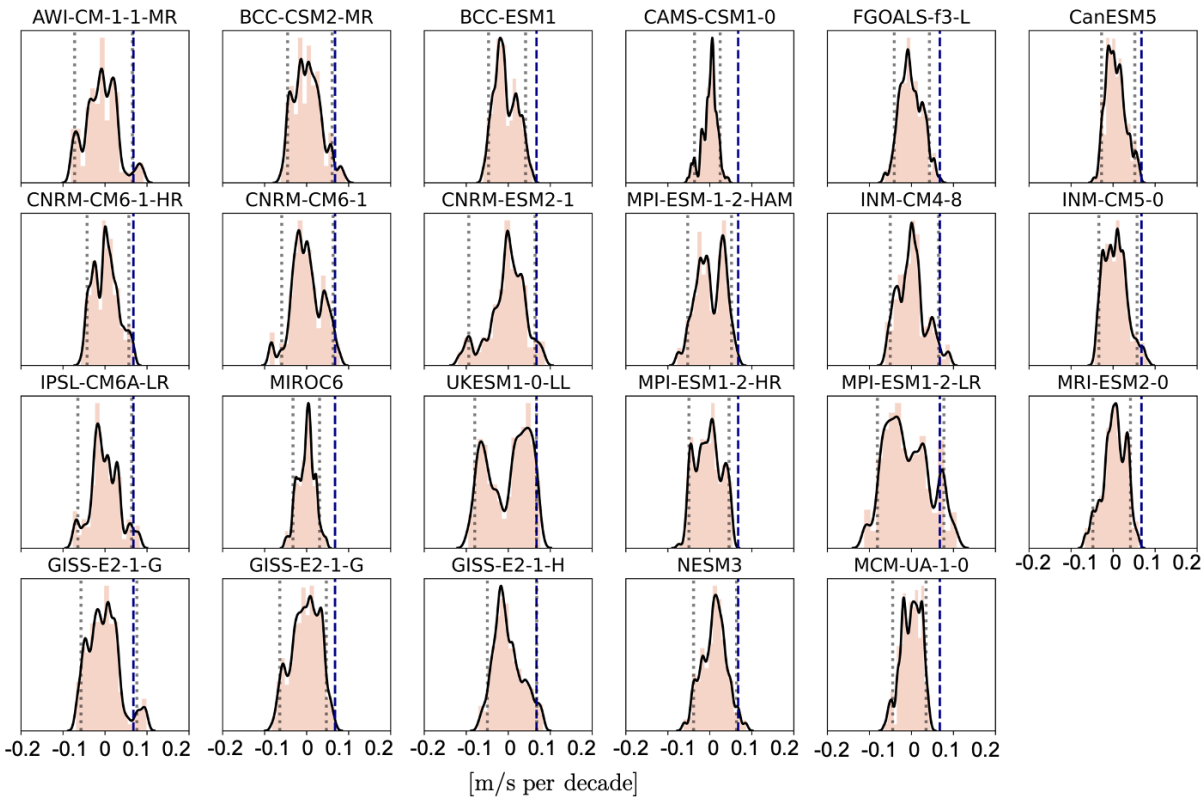

Figure S7 | Histogram represents the probability density function of 41-year annual mean trends in the zonal mean strength of SH westerlies calculated from the pre-industrial control simulations from 23 CMIP6 models (200 years for each model). Monte Carlo method is used to calculate the trend over a random chunk of 41 years of data from 200-year simulation of each model and the process is repeated 10,000 times for each model. Dashed blue line represents the trend calculated from ERA5 reanalysis over the current observational time period (1979-2019). Dotted black lines represent 5th and 95th percentile (i.e. bounds for 90% confidence) of the density function. The trends calculated from the reanalysis are significant at 90% confidence if the blue dashed line does not fall between the two dotted black lines.

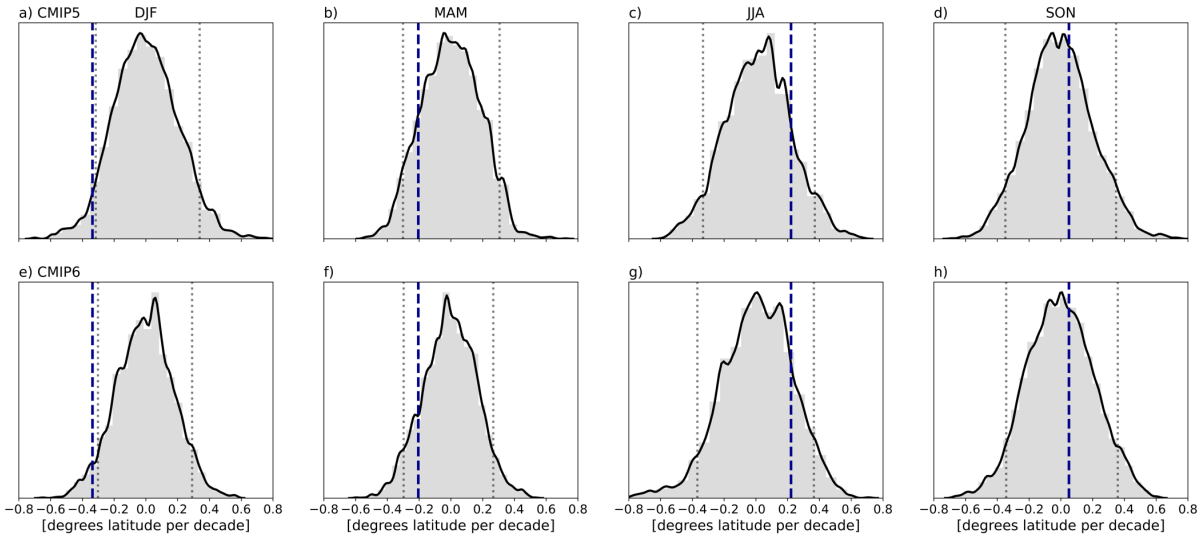

Figure S8 | Histogram represents the probability density function of 41-year trends in the zonal mean location of SH westerlies calculated from pre-industrial control simulations from 28 CMIP5 and 23 CMIP6 models (200 years for each model) for each season. Monte Carlo method is used to calculate the trend over a random chunk of 41 years of data from 200-year simulation of each model and the process is repeated 10,000 times for each model. All the 41-year trends from each model (10,000 for each model) are then concatenated and probability density function is plotted. Dashed blue line represents the trend calculated from ERA5 reanalysis over the current observational time period (1979-2019). Dotted black lines represent 5^{th} and 95^{th} percentile (i.e. bounds for 90% confidence) of the density function. The trends calculated from the reanalysis are significant at 90% confidence if the blue dashed line does not fall between the two dotted black lines.

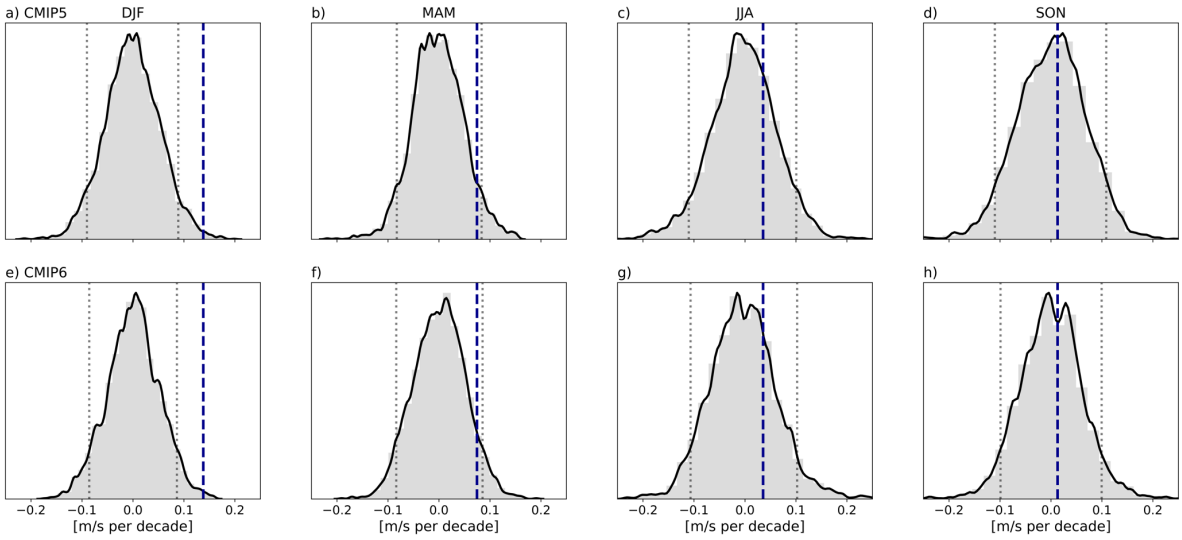

Figure S9 | Histogram represents the probability density function of 41-year trends in the zonal mean strength of SH westerlies calculated from pre-industrial control simulations from 28 CMIP5 and 23 CMIP6 models (200 years for each model) for each season. Monte Carlo method is used to calculate the trend over a random chunk of 41 years of data from 200-year simulation of each model and the process is repeated 10,000 times for each model. All the 41-year trends from each model (10,000 for each model) are then concatenated and probability density function is plotted. Dashed blue line represents the trend calculated from ERA5 reanalysis over the current observational time period (1979-2019). Dotted black lines represent 5^{th} and 95^{th} percentile (i.e. bounds for 90% confidence) of the density function. The trends calculated from the reanalysis are significant at 90% confidence if the blue dashed line does not fall between the two dotted black lines.

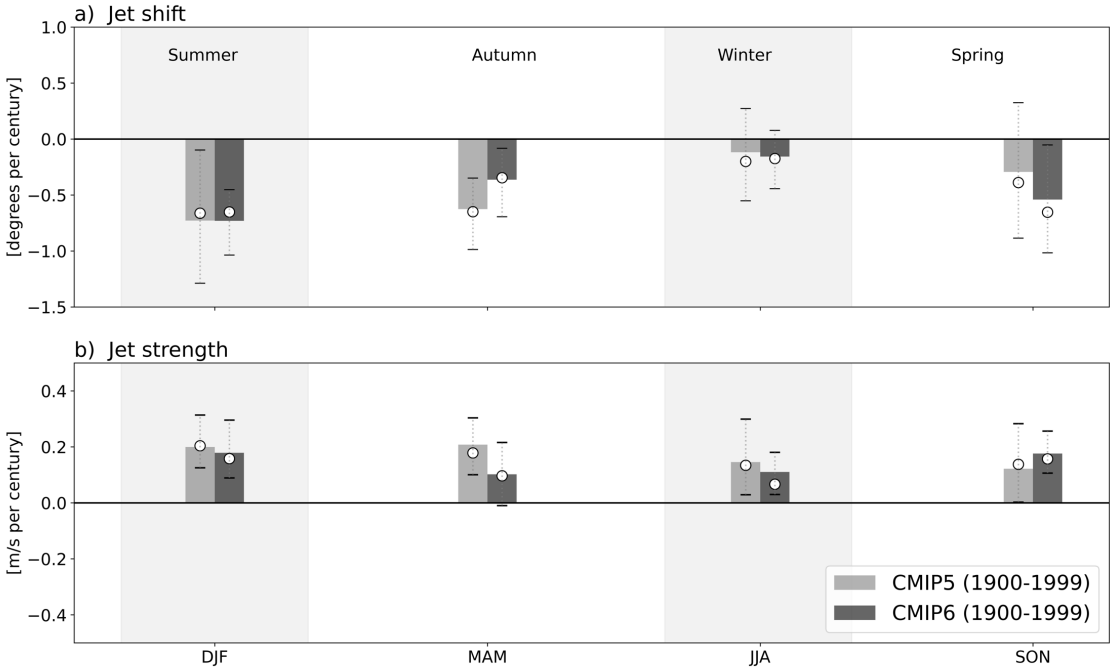

Figure S10 | Historical seasonal trends in position and strength in maximum zonal winds. Trends in maximum zonally averaged zonal wind latitude (panel a) strength (panel b) over historical (1900-1999) for CMIP5 and CMIP6 models. Colored bars represent multi-model mean trends, circles represent the multi-model median and dashed bars represent the inter-quartile range.

Table S1 | CMIP5 models used in the study. Models marked with asterisk are the models used for comparison between CMIP5 and CMIP models

Model	Modeling Center	Scenario			Ozone dataset reference	Main reference
		Historical	RCP4.5	RCP8.5		
CanESM2	Canadian Centre for Climate Modeling and Analysis, Canada	✓	✓	✓	(Cionni et al., 2011)	(von Salzen et al., 2013)
CMCC-CESM	Centro Euro-Mediterraneo sui Cambiamenti Climatici, Italy	✓		✓	(Cionni et al., 2011)	(Vichi et al., 2013)
CMCC-CM		✓	✓	✓	(Cionni et al., 2011)	(Vichi et al., 2013)
CMCC-CMS		✓	✓	✓	(Cionni et al., 2011)	(Vichi et al., 2013)
CNRM-CM5-2	Centre National de Recherches Meteorologiques, France	✓	-	-	(Cariolle & Teyssèdre, 2007)	(Voldoire et al., 2013)
CNRM-CM5		✓	-	-	(Cariolle & Teyssèdre, 2007)	(Voldoire et al., 2013)
INMCM4*	Russian Institute for Numerical Mathematics, Russia	✓	✓	✓	(Cionni et al., 2011)	(E M Volodin et al., 2010)
IPSL-CM5A-LR*	Institut Pierre Simon Laplace, France	✓	✓	✓	(Szopa et al., 2013)	(Dufresne et al., 2013)
IPSL-CM5A-MR		✓	✓	✓	(Szopa et al., 2013)	(Dufresne et al., 2013)
IPSL-CM5B-LR		✓	✓	✓	(Szopa et al., 2013)	(Dufresne et al., 2013)
MIROC-ESM-CHEM	Japan Agency for Marine-Earth Science and Technology, Atmosphere and Ocean Research Institute (The University of Tokyo), and National Institute for Environmental Studies, Japan	✓	✓	✓	(Watanabe et al., 2011)	(Watanabe et al., 2011)
MIROC-ESM		✓		✓	(Watanabe et al., 2011)	(Watanabe et al., 2011)
MIROC5*		✓	✓	✓	(Kawase et al., 2011)	(Watanabe et al., 2011)
HadGEM2-CC	Met Office Hadley Centre, UK	-	✓	✓	(Cionni et al., 2011; Jones et al., 2011)	(Martin et al., 2011)
HadGEM2-ES		-	✓	-	(Jones et al., 2011; O'Connor et al., 2014)	(Collins et al., 2011)
HadCM3		✓	-	-	(Cionni et al., 2011; Jones et al., 2011)	(Gordon et al., 2000)
HadGEM2-AO		✓	✓	✓	(Cionni et al., 2011; Jones et al., 2011)	(Martin et al., 2011)
MPI-ESM-LR*	Max Planck Institute for Meteorology, Germany	✓	-	-	(Cionni et al., 2011; Jones et al., 2011)	(Giorgetta et al., 2013)
MPI-ESM-MR*		✓	✓	✓	(Cionni et al., 2011; Jones et al., 2011)	(Giorgetta et al., 2013)
MPI-ESM-P		✓	-	-	(Cionni et al., 2011; Jones et al., 2011)	(Giorgetta et al., 2013)
MRI-CGCM3	Meteorological Research Institute, Japan Norwegian Climate Centre, Norway	✓	✓	✓	(Cionni et al., 2011)	(Yukimoto et al., 2012)
NorESM1-M*		✓	-	-	(Lamarque et al., 2010, 2012)	(Iversen et al., 2013)
NorESM1-ME		✓	✓		(Lamarque et al., 2010, 2012)	(Iversen et al., 2013)
MRI-ESM1*		✓	-	✓	(Cionni et al., 2011)	(Yukimoto et al., 2012)

GISS-E2-H-CC*	NASA Goddard Institute for Space Studies, USA	✓	✓	✓	(Shindell et al., 2013)	(Schmidt et al., 2006)
GISS-E2-H*		✓	✓	✓	(Hansen et al., 2007)	(Schmidt et al., 2006)
GISS-E2-R-CC		✓	✓	✓	(Shindell et al., 2013)	(Schmidt et al., 2006)
GISS-E2-R*		✓	✓	✓	(Hansen et al., 2007)	(Schmidt et al., 2006)
GFDL-CM2p1	NOAA Geophysical Fluid Dynamics Laboratory, USA	✓	-	-	(Austin & Wilson, 2006; Horowitz et al., 2003)	(Donner et al., 2011)
GFDL-CM3*		✓	✓	✓	(Cionni et al., 2011)	(Donner et al., 2011)
GFDL-ESM2G*		✓	✓	✓	(Cionni et al., 2011)	(Dunne et al., 2012)
GFDL-ESM2M		✓	✓	✓	(Cionni et al., 2011)	(Dunne et al., 2012)
ACCESS1-0	Centre for Australian Weather and Climate Research, Australia	✓	✓	✓	(Cionni et al., 2011)	(Dix et al., 2013)
ACCESS1-3		✓	✓	✓	(Cionni et al., 2011)	(Dix et al., 2013)
CSIRO-Mk-3-6-0	Commonwealth Scientific and Industrial Research Organization in collaboration with Queensland Climate Change Centre of Excellence, Australia	✓	✓	✓	(Cionni et al., 2011)	(Rotstayn et al., 2012)

Table S2 | CMIP6 models used in the study. Models marked with asterisk are the models used for comparison between CMIP5 and CMIP models

Model	Modeling Centre	Scenario			Main reference
		Historical	SSP2-4.5	SSP5-8.5	
AWI-CM-1-1-MR	Alfred Wegener Institute and Helmholtz Centre for Polar and Marine Research, Germany	-	✓	✓	(Semmler et al., 2020)
BCC-CSM2-MR	Beijing Climate Centre, China	✓	✓	✓	(Wu et al., 2019)
BCC-ESM1	Beijing Climate Centre, China	✓	-	-	(Wu et al., 2020)
CAMS-CSM1-0	Chinese Academy of Meteorological Sciences, China	✓	✓	✓	(Rong et al., 2018)
FGOALS-f3-L	Chinese Academy of Sciences, China	-	✓	✓	(He et al., 2019)
CanESM5	Canadian Centre for Climate Modelling and Analysis, Environment and Climate Change Canada, Canada	✓	✓	✓	(Swart et al., 2019)
CNRM-CM6-1-HR	CNRM (Centre National de Recherches Meteorologiques) and CERFACS (Centre Europeen de Recherche et de Formation Avancee en Calcul Scientifique), France	-	✓	✓	(Voldoire et al., 2019)
CNRM-CM6-1		-	✓	✓	(Voldoire et al., 2019)
CNRM-ESM2-1		-	✓		(Séférian et al., 2019)
MPI-ESM-1-2-HAM	ETH Zurich, Switzerland; Max Planck Institut fur Meteorologie, Germany; Forschungszentrum Julich, Germany; University of Oxford, UK; Finnish Meteorological Institute, Finland; Leibniz Institute for Tropospheric Research, Germany; Center for Climate Systems Modeling (C2SM) at ETH Zurich, Switzerland	✓	✓	✓	(Gutjahr et al., 2019)
INM-CM4-8*	Institute for Numerical Mathematics, Russian Academy of Science, Russia	✓	✓	✓	(Evgenii M Volodin et al., 2018)
INM-CM5-0		✓	✓	✓	(E. Volodin & Gritsun, 2018)
IPSL-CM6A-LR*	Institut Pierre Simon Laplace, France	✓	✓	✓	(Boucher et al., 2020)
MIROC6*	JAMSTEC (Japan Agency for Marine-Earth Science and Technology, Japan), AORI (Atmosphere and Ocean Research Institute, The University of Tokyo, Japan), NIES (National Institute for Environmental Studies, Japan), and R-CCS (RIKEN Centre for Computational Science, Japan)	✓	✓	✓	(Tatebe et al., 2019)
MPI-ESM1-2-HR*	Max Planck Institute for Meteorology, Germany; Deutsches Klimarechenzentrum, Germany; Deutscher Wetterdienst, Germany	✓	✓	✓	(Gutjahr et al., 2019)
MPI-ESM1-2-LR*	Max Planck Institute for Meteorology, Germany and Alfred Wegener Institute and Helmholtz Centre for Polar and Marine Research, Germany	✓	✓	✓	(Mauritsen et al., 2019)
MRI-ESM2-0*	Meteorological Research Institute, Japan	✓	✓	-	(Yukimoto et al., 2019)
GISS-E2-1-G-CC*	NASA-GISS (Goddard Institute for Space Studies), USA	✓	-	-	(Bauer et al., 2020)
GISS-E2-1-G*		✓	-	-	
GISS-E2-1-H*		✓	-	-	

NorCPM1*	NorESM Climate modeling Consortium consisting of CICERO (Center for International Climate and Environmental Research), MET-Norway (Norwegian Meteorological Institute), NERSC (Nansen Environmental and Remote Sensing Center), NILU (Norwegian Institute for Air Research), UiB (University of Bergen), UiO (University of Oslo) and UNI (Uni Research), Norway	✓	-	-	(Li et al., 2019)
KACE-1-0-G	National Institute of Meteorological Sciences/Korea Meteorological Administration, Climate Research Division, Republic of Korea	✓	-	-	(Lee et al., 2020)
GFDL-CM4*	National Oceanic and Atmospheric Administration, Geophysical Fluid Dynamics Laboratory, USA	✓	✓	✓	(Held et al., 2019)
GFDL-ESM4*		✓	✓	✓	(Krasting et al., 2018)
NESM3	Nanjing University of Information Science and Technology, China	✓	✓	✓	(Cao et al., 2018)
MCM-UA-1-0	Department of Geosciences, University of Arizona, USA	✓	✓	✓	(Stouffer, 2019)
UKESM1-0-LL	Met Office Hadley Centre, UK; Natural Environment Research Council, UK; National Institute of Meteorological Sciences/Korea Meteorological Administration, Republic of Korea; National Institute of Water and Atmospheric Research, New Zealand	-	✓	✓	(Sellar et al., 2019)

Table S3 | Annual and seasonal trends in the westerly jet shift and strength during the 20th and 21st Century in CMIP5 and CMIP6 models. Trends are shown as multi-model mean trend ± one standard deviation. Trends are represented from CMIP5 models (not inside brackets) and from CMIP6 models (inside brackets). Trends in red are from 2000-2099 in RCP8.5 (CMIP5) and SSP5-8.5 (CMIP6) and in blue from 2000-2099 in RCP4.5 (CMIP5) and SSP2-4.5 (CMIP6). Bold values represent trends which are significant at 95% confidence level.

		Annual	DJF	MAM	JJA	SON
1900-1999	Shift (°latitude)	**-0.47 ± 0.37** **(-0.46 ± 0.36)**	**-0.73 ± 0.7** **(-0.73 ± 0.53)**	**-0.63 ± 0.55** **(-0.36 ± 0.49)**	-0.12 ± 0.58 (-0.16 ± 0.47)	**-0.29 ± 0.71** **(-0.54 ± 0.77)**
	Strength (m/s)	**0.17 ± 0.08** **(0.14 ± 0.09)**	**0.2 ± 0.15** **(0.18 ± 0.15)**	**(0.21 ± 0.14)** **(0.10 ± 0.15)**	**0.15 ± 0.16** **0.11 ± 0.13**	**0.12 ± 0.21** **(0.18 ± 0.15)**
2000-2099	Shift (°latitude)	**-1.62 ± 0.86** **(-1.54 ± 0.82)** -0.56 ± 0.89 (-0.46 ± 0.99)	**-1.9 ± 1.22** **(-1.18 ± 1.02)** -0.42 ± 1.29 (0.25 ± 1.85)	**-2.24 ± 1.22** **(-1.45 ± 1.25)** **-0.85 ± 0.92** -0.28 ± 1.38	**-0.7 ± 1.05** (-0.31 ± 1.17) -0.28 ± 0.97 (-0.16 ± 0.99)	**-0.81 ± 1.2** -0.07 ± 1.6 -0.11 ± 1.09 0.15 ± 1.34
	Strength (m/s)	**0.79 ± 0.52** **(0.66 ± 0.46)** 0.24 ± 0.37 (0.21 ± 0.46)	**0.49 ± 0.56** **(0.47 ± 0.43)** 0.08 ± 0.48 0.12 ± 0.39	**0.70 ± 0.51** **(0.68 ± 0.43)** **0.25 ± 0.50** **(0.22 ± 0.48)**	**0.83 ± 0.6** **(0.74 ± 0.64)** **0.34 ± 0.46** (0.23 ± 0.62)	**0.82 ± 0.60** **0.74 ± 0.53** **0.24 ± 0.47** **0.27 ± 0.50**

References

Austin, J., & Wilson, R. J. (2006). Ensemble simulations of the decline and recovery of stratospheric ozone. *Journal of Geophysical Research: Atmospheres*, *111*(D16). https://doi.org/10.1029/2005JD006907

Bauer, S. E., Tsigaridis, K., Faluvegi, G., Kelley, M., Lo, K. K., Miller, R. L., et al. (2020). Historical (1850-2014) aerosol evolution and role on climate forcing using the GISS ModelE2.1 contribution to CMIP6. *Journal of Advances in Modeling Earth Systems*, e2019MS001978. https://doi.org/10.1029/2019MS001978

Boucher, O., Servonnat, J., Albright, A. L., Aumont, O., Balkanski, Y., Bastrikov, V., et al. (2020). Presentation and evaluation of the IPSL-CM6A-LR climate model. *Journal of Advances in Modeling Earth Systems*, e2019MS002010. https://doi.org/10.1029/2019MS002010

Cao, J., Wang, B., Yang, Y.-M., Ma, L., Li, J., Sun, B., et al. (2018). The NUIST Earth System Model (NESM) version 3: description and preliminary evaluation. *Geosci. Model Dev.*, *11*(7), 2975–2993. https://doi.org/10.5194/gmd-11-2975-2018

Cariolle, D., & Teyssèdre, H. (2007). A revised linear ozone photochemistry parameterization for use in transport and general circulation models: multi-annual simulations. *Atmos. Chem. Phys.*, *7*(9), 2183–2196. https://doi.org/10.5194/acp-7-2183-2007

Cionni, I., Eyring, V., Lamarque, J. F., Randel, W. J., Stevenson, D. S., Wu, F., et al. (2011). Ozone database in support of CMIP5 simulations: Results and corresponding radiative forcing. *Atmospheric Chemistry and Physics*, *11*(21), 11267–11292. https://doi.org/10.5194/acp-11-11267-2011

Collins, W. J., Bellouin, N., Doutriaux-Boucher, M., Gedney, N., Halloran, P., Hinton, T., et al. (2011). Development and evaluation of an Earth-System model – HadGEM2. *Geosci.*

Model Dev., *4*(4), 1051–1075. https://doi.org/10.5194/gmd-4-1051-2011

Dix, M., Vohralik, P., Bi, D., Rashid, H., Marsland, S., O'Farrell, S., et al. (2013). The ACCESS coupled model: Documentation of core CMIP5 simulations and initial results. *Australian Meteorological and Oceanographic Journal*, *63*(1), 83–99. https://doi.org/10.22499/2.6301.006

Donner, L. J., Wyman, B. L., Hemler, R. S., Horowitz, L. W., Ming, Y., Zhao, M., et al. (2011). The Dynamical Core, Physical Parameterizations, and Basic Simulation Characteristics of the Atmospheric Component AM3 of the GFDL Global Coupled Model CM3. *Journal of Climate*, *24*(13), 3484–3519. https://doi.org/10.1175/2011JCLI3955.1

Dufresne, J.-L., Foujols, M.-A., Denvil, S., Caubel, A., Marti, O., Aumont, O., et al. (2013). Climate change projections using the IPSL-CM5 Earth System Model: from CMIP3 to CMIP5. *Climate Dynamics*, *40*(9), 2123–2165. https://doi.org/10.1007/s00382-012-1636-1

Dunne, J. P., John, J. G., Adcroft, A. J., Griffies, S. M., Hallberg, R. W., Shevliakova, E., et al. (2012). GFDL's ESM2 Global Coupled Climate–Carbon Earth System Models. Part I: Physical Formulation and Baseline Simulation Characteristics. *Journal of Climate*, *25*(19), 6646–6665. https://doi.org/10.1175/JCLI-D-11-00560.1

Giorgetta, M. A., Jungclaus, J., Reick, C. H., Legutke, S., Bader, J., Böttinger, M., et al. (2013). Climate and carbon cycle changes from 1850 to 2100 in MPI-ESM simulations for the Coupled Model Intercomparison Project phase 5. *Journal of Advances in Modeling Earth Systems*, *5*(3), 572–597. https://doi.org/10.1002/jame.20038

Gordon, C., Cooper, C., Senior, C. A., Banks, H., Gregory, J. M., Johns, T. C., et al. (2000). The simulation of SST, sea ice extents and ocean heat transports in a version of the Hadley Centre coupled model without flux adjustments. *Climate Dynamics*, *16*(2), 147–168.

https://doi.org/10.1007/s003820050010

Gutjahr, O., Putrasahan, D., Lohmann, K., Jungclaus, J. H., von Storch, J.-S., Brüggemann, N., et al. (2019). Max Planck Institute Earth System Model (MPI-ESM1.2) for the High-Resolution Model Intercomparison Project (HighResMIP). *Geosci. Model Dev.*, *12*(7), 3241–3281. https://doi.org/10.5194/gmd-12-3241-2019

Hansen, J., Sato, M., Ruedy, R., Kharecha, P., Lacis, A., Miller, R., et al. (2007). Climate simulations for 1880–2003 with GISS modelE. *Climate Dynamics*, *29*(7), 661–696. https://doi.org/10.1007/s00382-007-0255-8

He, B., Bao, Q., Wang, X., Zhou, L., Wu, X., Liu, Y., et al. (2019). CAS FGOALS-f3-L Model Datasets for CMIP6 Historical Atmospheric Model Intercomparison Project Simulation. *Advances in Atmospheric Sciences*, *36*(8), 771–778. https://doi.org/10.1007/s00376-019-9027-8

Held, I. M., Guo, H., Adcroft, A., Dunne, J. P., Horowitz, L. W., Krasting, J., et al. (2019). Structure and Performance of GFDL's CM4.0 Climate Model. *Journal of Advances in Modeling Earth Systems*, *11*(11), 3691–3727. https://doi.org/10.1029/2019MS001829

Horowitz, L. W., Walters, S., Mauzerall, D. L., Emmons, L. K., Rasch, P. J., Granier, C., et al. (2003). A global simulation of tropospheric ozone and related tracers: Description and evaluation of MOZART, version 2. *Journal of Geophysical Research: Atmospheres*, *108*(D24). https://doi.org/10.1029/2002JD002853

Iversen, T., Bentsen, M., Bethke, I., Debernard, J. B., Kirkevåg, A., Seland, Ø., et al. (2013). The Norwegian Earth System Model, NorESM1-M – Part 2: Climate response and scenario projections. *Geosci. Model Dev.*, *6*(2), 389–415. https://doi.org/10.5194/gmd-6-389-2013

Jones, C. D., Hughes, J. K., Bellouin, N., Hardiman, S. C., Jones, G. S., Knight, J., et al. (2011).

The HadGEM2-ES implementation of CMIP5 centennial simulations. *Geosci. Model Dev.*, *4*(3), 543–570. https://doi.org/10.5194/gmd-4-543-2011

Kawase, H., Nagashima, T., Sudo, K., & Nozawa, T. (2011). Future changes in tropospheric ozone under Representative Concentration Pathways (RCPs). *Geophysical Research Letters*, *38*(5). https://doi.org/10.1029/2010GL046402

Krasting, J. P., John, J. G., Blanton, C., McHugh, C., Nikonov, S., Radhakrishnan, A., et al. (2018). NOAA-GFDL GFDL-ESM4 model output prepared for CMIP6 CMIP historical. Earth System Grid Federation. https://doi.org/10.22033/ESGF/CMIP6.8597

Lamarque, J.-F., Bond, T. C., Eyring, V., Granier, C., Heil, A., Klimont, Z., et al. (2010). Historical (1850–2000) gridded anthropogenic and biomass burning emissions of reactive gases and aerosols: methodology and application. *Atmos. Chem. Phys.*, *10*(15), 7017–7039. https://doi.org/10.5194/acp-10-7017-2010

Lamarque, J.-F., Emmons, L. K., Hess, P. G., Kinnison, D. E., Tilmes, S., Vitt, F., et al. (2012). CAM-chem: description and evaluation of interactive atmospheric chemistry in the Community Earth System Model. *Geosci. Model Dev.*, *5*(2), 369–411. https://doi.org/10.5194/gmd-5-369-2012

Lee, J., Kim, J., Sun, M.-A., Kim, B.-H., Moon, H., Sung, H. M., et al. (2020). Evaluation of the Korea Meteorological Administration Advanced Community Earth-System model (K-ACE). *Asia-Pacific Journal of Atmospheric Sciences*, *56*(3), 381–395. https://doi.org/10.1007/s13143-019-00144-7

Li, F., Orsolini, Y. J., Keenlyside, N., Shen, M.-L., Counillon, F., & Wang, Y. G. (2019). Impact of Snow Initialization in Subseasonal-to-Seasonal Winter Forecasts With the Norwegian Climate Prediction Model. *Journal of Geophysical Research: Atmospheres*, *124*(17–18), 10033–10048. https://doi.org/10.1029/2019JD030903

Martin, G. M., Bellouin, N., Collins, W. J., Culverwell, I. D., Halloran, P. R., Hardiman, S. C., et al. (2011). The HadGEM2 family of Met Office Unified Model climate configurations. *Geoscientific Model Development*, *4*(3), 723–757. https://doi.org/10.5194/gmd-4-723-2011

Mauritsen, T., Bader, J., Becker, T., Behrens, J., Bittner, M., Brokopf, R., et al. (2019). Developments in the MPI-M Earth System Model version 1.2 (MPI-ESM1.2) and Its Response to Increasing CO2. *Journal of Advances in Modeling Earth Systems*, *11*(4), 998–1038. https://doi.org/10.1029/2018MS001400

O'Connor, F. M., Johnson, C. E., Morgenstern, O., Abraham, N. L., Braesicke, P., Dalvi, M., et al. (2014). Evaluation of the new UKCA climate-composition model – Part 2: The Troposphere. *Geosci. Model Dev.*, *7*(1), 41–91. https://doi.org/10.5194/gmd-7-41-2014

Rong, X., Li, J., Chen, H., Xin, Y., Su, J., Hua, L., et al. (2018). The CAMS Climate System Model and a Basic Evaluation of Its Climatology and Climate Variability Simulation. *Journal of Meteorological Research*, *32*(6), 839–861. https://doi.org/10.1007/s13351-018-8058-x

Rotstayn, L. D., Jeffrey, S. J., Collier, M. A., Dravitzki, S. M., Hirst, A. C., Syktus, J. I., & Wong, K. K. (2012). Aerosol- and greenhouse gas-induced changes in summer rainfall and circulation in the Australasian region: a study using single-forcing climate simulations. *Atmos. Chem. Phys.*, *12*(14), 6377–6404. https://doi.org/10.5194/acp-12-6377-2012

von Salzen, K., Scinocca, J. F., McFarlane, N. A., Li, J., Cole, J. N. S., Plummer, D., et al. (2013). The Canadian Fourth Generation Atmospheric Global Climate Model (CanAM4). Part I: Representation of Physical Processes. *Atmosphere-Ocean*, *51*(1), 104–125. https://doi.org/10.1080/07055900.2012.755610

Schmidt, G. A., Ruedy, R., Hansen, J. E., Aleinov, I., Bell, N., Bauer, M., et al. (2006). Present-Day Atmospheric Simulations Using GISS ModelE: Comparison to In Situ, Satellite, and

Reanalysis Data. *Journal of Climate*, *19*(2), 153–192. https://doi.org/10.1175/JCLI3612.1

Séférian, R., Nabat, P., Michou, M., Saint-Martin, D., Voldoire, A., Colin, J., et al. (2019). Evaluation of CNRM Earth System Model, CNRM-ESM2-1: Role of Earth System Processes in Present-Day and Future Climate. *Journal of Advances in Modeling Earth Systems*, *11*(12), 4182–4227. https://doi.org/10.1029/2019MS001791

Sellar, A. A., Jones, C. G., Mulcahy, J. P., Tang, Y., Yool, A., Wiltshire, A., et al. (2019). UKESM1: Description and Evaluation of the U.K. Earth System Model. *Journal of Advances in Modeling Earth Systems*, *11*(12), 4513–4558. https://doi.org/10.1029/2019MS001739

Semmler, A.-T., Danilov, S., Gierz, P., Goessling, H., Hegewald, J., Hinrichs, C., et al. (2020). Simulations for CMIP6 with the AWI climate model AWI-CM-1-1. *Earth and Space Science Open Archive*. https://doi.org/10.1002/essoar.10501538.1

Shindell, D. T., Pechony, O., Voulgarakis, A., Faluvegi, G., Nazarenko, L., Lamarque, J.-F., et al. (2013). Interactive ozone and methane chemistry in GISS-E2 historical and future climate simulations. *Atmos. Chem. Phys.*, *13*(5), 2653–2689. https://doi.org/10.5194/acp-13-2653-2013

Stouffer, R. (2019). U of Arizona MCM-UA-1-0 model output prepared for CMIP6 CMIP. Earth System Grid Federation. https://doi.org/10.22033/ESGF/CMIP6.2421

Swart, N. C., Cole, J. N. S., Kharin, V. V, Lazare, M., Scinocca, J. F., Gillett, N. P., et al. (2019). The Canadian Earth System Model version 5 (CanESM5.0.3). *Geosci. Model Dev.*, *12*(11), 4823–4873. https://doi.org/10.5194/gmd-12-4823-2019

Szopa, S., Balkanski, Y., Schulz, M., Bekki, S., Cugnet, D., Fortems-Cheiney, A., et al. (2013). Aerosol and ozone changes as forcing for climate evolution between 1850 and 2100.

Climate Dynamics, *40*(9), 2223–2250. https://doi.org/10.1007/s00382-012-1408-y

Tatebe, H., Ogura, T., Nitta, T., Komuro, Y., Ogochi, K., Takemura, T., et al. (2019). Description and basic evaluation of simulated mean state, internal variability, and climate sensitivity in MIROC6. *Geosci. Model Dev.*, *12*(7), 2727–2765. https://doi.org/10.5194/gmd-12-2727-2019

Vichi, M., Navarra, A., & Fogli, P. G. (2013). Adjustment of the natural ocean carbon cycle to negative emission rates. *Climatic Change*, *118*(1), 105–118. https://doi.org/10.1007/s10584-012-0677-0

Voldoire, A., Sanchez-Gomez, E., Salas y Mélia, D., Decharme, B., Cassou, C., Sénési, S., et al. (2013). The CNRM-CM5.1 global climate model: description and basic evaluation. *Climate Dynamics*, *40*(9), 2091–2121. https://doi.org/10.1007/s00382-011-1259-y

Voldoire, A., Saint-Martin, D., Sénési, S., Decharme, B., Alias, A., Chevallier, M., et al. (2019). Evaluation of CMIP6 DECK Experiments With CNRM-CM6-1. *Journal of Advances in Modeling Earth Systems*, *11*(7), 2177–2213. https://doi.org/10.1029/2019MS001683

Volodin, E., & Gritsun, A. (2018). Simulation of observed climate changes in 1850-2014 with climate model INM-CM5. *Earth System Dynamics*, *9*(4), 1235–1242. https://doi.org/10.5194/esd-9-1235-2018

Volodin, E M, Dianskii, N. A., & Gusev, A. V. (2010). Simulating present-day climate with the INMCM4.0 coupled model of the atmospheric and oceanic general circulations. *Izvestiya, Atmospheric and Oceanic Physics*, *46*(4), 414–431. https://doi.org/10.1134/S000143381004002X

Volodin, Evgenii M, Mortikov, E. V, Kostrykin, S. V, Galin, V. Y., Lykossov, V. N., Gritsun, A. S., et al. (2018). Simulation of the modern climate using the INM-CM48 climate model. *Russian Journal of Numerical Analysis and Mathematical Modelling*, *33*(6), 367–374.

https://doi.org/https://doi.org/10.1515/rnam-2018-0032

Watanabe, S., Hajima, T., Sudo, K., Nagashima, T., Takemura, T., Okajima, H., et al. (2011). MIROC-ESM 2010: model description and basic results of CMIP5-20c3m experiments. *Geosci. Model Dev.*, *4*(4), 845–872. https://doi.org/10.5194/gmd-4-845-2011

Wu, T., Lu, Y., Fang, Y., Xin, X., Li, L., Li, W., et al. (2019). The Beijing Climate Center Climate System Model (BCC-CSM): The main progress from CMIP5 to CMIP6. *Geoscientific Model Development*, *12*(4), 1573–1600. https://doi.org/10.5194/gmd-12-1573-2019

Wu, T., Zhang, F., Zhang, J., Jie, W., Zhang, Y., Wu, F., et al. (2020). Beijing Climate Center Earth System Model version 1 (BCC-ESM1): Model description and evaluation of aerosol simulations. *Geoscientific Model Development*, *13*(3), 977–1005. https://doi.org/10.5194/gmd-13-977-2020

Yukimoto, S., Adachi, Y., Hosaka, M., Tomonori, S., Yoshimura, H., Hirabara, M., et al. (2012). A New Global Climate Model of the Meteorological Research Institute: MRI-CGCM3: Model Description and Basic Performance. *Journal of the Meteorological Society of Japan*, *90A*, 23–64. https://doi.org/10.2151/jmsj.2012-A02

Yukimoto, S., Hideaki, K., Koshiro, T., Oshima, N., Yoshida, K., Urakawa, S., et al. (2019). The Meteorological Research Institute Earth System Model Version 2.0, MRI-ESM2.0: Description and Basic Evaluation of the Physical Component. *Journal of the Meteorological Society of Japan. Ser. II*, *advpub*. https://doi.org/10.2151/jmsj.2019-051